MATHEMATICAL BIOSCIENCES
AND ENGINEERING
Volume **9**, Number **4**, October **2012**

doi:10.3934/mbe.2012.9.915

pp. **915–935**

# BASIC STOCHASTIC MODELS FOR VIRAL INFECTION WITHIN A HOST

Sukhitha W. Vidurupola and Linda J. S. Allen

Texas Tech University
Department of Mathematics and Statistics
Lubbock, Texas 79409-1042, USA

(Communicated by Yang Kuang)

Abstract. Stochastic differential equation (SDE) models are formulated for intra-host virus-cell dynamics during the early stages of viral infection, prior to activation of the immune system. The SDE models incorporate more realism into the mechanisms for viral entry and release than ordinary differential equation (ODE) models and show distinct differences from the ODE models. The variability in the SDE models depends on the concentration, with much greater variability for small concentrations than large concentrations. In addition, the SDE models show significant variability in the timing of the viral peak. The viral peak is earlier for viruses that are released from infected cells via bursting rather than via budding from the cell membrane.

1. **Introduction.** Viruses require host cells in order to reproduce. Human immunodeficiency virus (HIV), the virus that causes AIDS, reproduces within the cells of the immune system, CD4+ T helper cells [36]. Human and avian influenza viruses reproduce in the cells of the respiratory epithelium [20]. Hantaviruses, the cause of hantavirus pulmonary syndrome, reproduce primarily in the vascular endothelial cells but also infect other cells [10, 38]. After viral entry into a host cell, a complex set of intracellular processes occur: transcription, translation, replication, assembly and release.

Some basic mathematical models of viral dynamics concentrate on two steps in this process: viral entry and release. One of the most well-known models for viral dynamics includes only three variables, one variable for free virus particles or virions, a second variable for healthy target cells, and a third variable for actively infected target cells [21, 25, 36]. Another basic model includes four variables; the fourth variable represents latently infected cells [24, 26]. These basic models are deterministic and describe the early stages of intra-host viral infection, prior to activation of the immune response.

Several stochastic models have been developed from these basic models and applied to HIV-1 [5, 12, 23, 29, 31, 30, 37]. Tuckwell and Le Corfec [31] developed one of the first stochastic models for intra-host viral infection in the form of stochastic differential equations (SDEs). Their deterministic skeleton has latently infected

2000 *Mathematics Subject Classification.* Primary: 92D30; Secondary: 34D20; 60H10.
*Key words and phrases.* Target cells, virus, stochastic differential equations.
Partial support was provided by the NSF grant # DMS-0718302 and the Fogarty International Center grant # R01TW006986-02 under the NIH NSF Ecology of Infectious Diseases initiative.

target cells. The SDE model shows the variability in the timing of the peak level of infection when a small amount of virus is introduced. The SDE model developed by Tuckwell and Le Corfec incorporated stochasticity only in the collisions and binding of virus particles to receptors on target cells. Tuckwell and Wan [30] formulated the backward Kolmogorov differential equations for this SDE model, useful in first passage time problems. Kamina et al. [12] developed another stochastic approach to the basic model with four variables, assuming Poisson, binomial and multinomial distributions for some of the processes. Tan and Wu [29] used extensive Monte Carlo simulations to study the distributions of the CD4+ T cells and virions in a stochastic version of the basic model with four variables. Chao et al. [5] used the basic virus-cell model as a starting point but formulated and simulated a more realistic multi-stage-structured model that includes cytotoxic T cell response, an agent-based model. Time is divided into fixed intervals so that after a fixed time interval, cells divide or transition to another stage dependent on a given probability distribution. The multiple stages account for the delays in reproduction and stimulation by the immune response. Yuan and Allen [37] derived Itô SDEs and continuous-time Markov chain models for the model with three variables, $T$, $I$, and $V$ and for a model that includes an immune response, applicable to HIV-1. Yuan and Allen [37] and Pearson et al. [23] applied a stochastic approximation to compute the probability of viral extinction for the budding and bursting release strategies.

Our goal in this investigation is to extend the work of Yuan and Allen [37], to derive Itô SDEs for the basic model with four variables, similar to Tuckwell and Le Corfec [31] but to include the variability due to births and deaths and the difference in viral release strategy. We investigate the dynamics of the Itô SDEs by obtaining differential equations for the moments of the joint probability density function. Numerical simulations illustrate the variability in the sample paths with different concentration or volumes, applicable to *in vivo* or *in vitro* studies. In addition, the variability in the peak viral load is shown to depend on the particular release strategy.

In Sections 2 and 3, the ODE and SDE models are introduced and some of their dynamics summarized. Numerical examples comparing the dynamics of the ODE and SDE models are presented in Section 4.

## 2. Model formulation.

### 2.1. ODE model.

The basic deterministic model is a system of four ODEs [24, 26]. Figure 1 is a compartmental diagram illustrating the dynamics of $T$ = healthy target cells, $L$ = latently infected cells, $I$ = actively infected cells and $V$ = virions. Only the actively infected cells reproduce virions that either lyse the cell or bud from the cell membrane. The model takes the form:

$$\begin{aligned}
\dot{T} &= \lambda - \mu T + rT\left[1 - \left(\frac{T+L+I}{T_{\max}}\right)\right] - kTV \\
\dot{L} &= pkTV - \mu L - \alpha L \\
\dot{I} &= (1-p)kTV + \alpha L - aI \\
\dot{V} &= NaI - \gamma V - kTV
\end{aligned} \tag{1}$$

A summary of the parameters is given in Table 1. All parameters are positive, unless noted otherwise. The parameters $r$ and $\lambda$ can be combined into one term

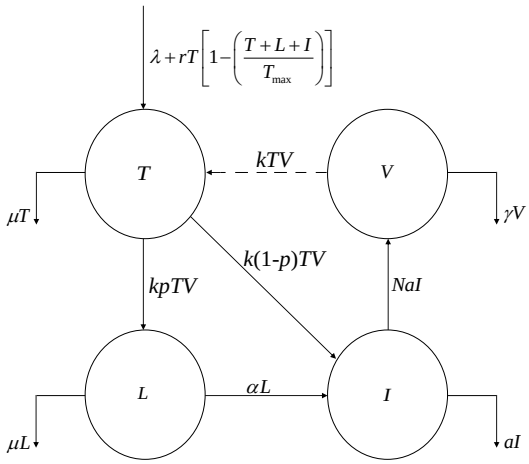


FIGURE 1. Compartmental diagram for the basic intra-host viral dynamics

TABLE 1. Description of parameters

| Parameters | Description |
|---|---|
| $\lambda$ | Rate of formation of new target cells |
| $r$ | Maximum rate of growth of target cells from viral stimulation |
| $T_{max}$ | Maximum target cell population |
| $\mu$ | Death rate of uninfected and latently infected target cells |
| $a$ | Death rate of actively infected target cell population |
| $\gamma$ | Death rate of virions |
| $k$ | Rate constant for healthy target cells becoming infected by virions |
| $\alpha$ | Rate latently infected cells convert to actively infected cells |
| $N$ | Number of virions produced from an infected cell=burst size |
| $p$ | Proportion of infected cells which are latent |

but we keep them separate as in models for HIV-1. For HIV-1, healthy T cells are reproduced in the thymus at a rate $\lambda$ and die at a per capita rate $\mu$. The term

$$rT\left[1-\left(\frac{T+L+I}{T_{\max}}\right)\right]$$

represents viral stimulation, a logistic type growth rate dependent on cell density, with a bound on the maximum population density, $T_{\max}$.

A mass action term is used to represent infection of the healthy T cells by a virion, $kTV$ (representing a loss of a healthy T cell and a loss of a free viral particle). A proportion $p$ of the infected T cells become latent and the remaining proportion $1-p$ become active. Latently infected T cells die at the same per capita rate $\mu$ as healthy T cells, then convert to actively infected T cells at a per capita rate $\alpha$. Actively infected T cells die at a per capita rate $a$. A reasonable assumption is that infected T cells have a higher death rate than healthy or latent T cells [24]:

$$a > \mu. \tag{2}$$

Prior to dying, actively infected T cells reproduce on average $N$ virions. The parameter $N$ is referred to as the "burst size" [24]. In addition, we assume for $r > 0$ that

$$\frac{\lambda}{\mu} < T_{\max}; \tag{3}$$

stimulation increases the T cell population.

A special case of this ODE model is when $r = 0$ in (1), applicable to viral infections where the target cells are not subject to antigenic stimulation. Tuckwell and Le Corfec [31] formulated an SDE model based on the underlying ODE model with $r = 0$.

### 2.2. **SDE models.**

2.2.1. *Bursting.* In the bursting case, an infected cell lyses and a burst of free virions is released. That is, one infected cell dies at the same time $N$ virions are released, $N \geq 2$. To differentiate the continuous random variables of the stochastic model from the deterministic variables, the continuous random variables for the four states $T$, $L$, $I$ and $V$ are denoted as $X_1$, $X_2$, $X_3$ and $X_4$, respectively. In addition, $X_{tot} = X_1 + X_2 + X_3$. These random variables are defined on an appropriately defined sample space $\Omega$, where $X_i(t) = X_i(\omega, t)$, $\omega \in \Omega$, with values for a fixed $t$ in the set $[0, \infty)$.

To formulate a system of Itô SDEs, the possible changes that occur in a discrete-time process are defined [1, 2, 8]. Let $\Delta X_i = X_i(t + \Delta t) - X_i(t)$. The possible changes in the vector $\vec{X} = [X_1, X_2, X_3, X_4]^{tr}$ for a small time interval $\Delta t$ and the corresponding probabilities are summarized in Table 2. (The superscript $tr$ refers to the transpose of a vector or a matrix.)

TABLE 2. Possible state changes in the case of bursting during the time interval $\Delta t$, where $X_i = X_i(t)$, $i = 1, 2, 3, 4$.

| $i$ | Change, $(\Delta\vec{X})_i$ | Probability, $p_i \Delta t$ |
|---|---|---|
| 1 | $(\Delta\vec{X})_1 = [1, 0, 0, 0]^{tr}$ | $\left[\lambda + rX_1\left(1 - \frac{X_{tot}}{T_{\max}}\right)\right]\Delta t$ |
| 2 | $(\Delta\vec{X})_2 = [-1, 0, 0, 0]^{tr}$ | $\mu X_1 \Delta t$ |
| 3 | $(\Delta\vec{X})_3 = [-1, 1, 0, -1]^{tr}$ | $pkX_1X_4\Delta t$ |
| 4 | $(\Delta\vec{X})_4 = [-1, 0, 1, -1]^{tr}$ | $(1-p)kX_1X_4\Delta t$ |
| 5 | $(\Delta\vec{X})_5 = [0, -1, 0, 0]^{tr}$ | $\mu X_2 \Delta t$ |
| 6 | $(\Delta\vec{X})_6 = [0, -1, 1, 0]^{tr}$ | $\alpha X_2 \Delta t$ |
| 7 | $(\Delta\vec{X})_7 = [0, 0, -1, N]^{tr}$ | $aX_3\Delta t$ |
| 8 | $(\Delta\vec{X})_8 = [0, 0, 0, -1]^{tr}$ | $\gamma X_4 \Delta t$ |
| 9 | $(\Delta\vec{X})_9 = [0, 0, 0, 0]^{tr}$ | $1 - \sum_{i=1}^{8} p_i \Delta t$ |

The change $(\Delta\vec{X})_1$ represents a birth of a healthy T cell, whereas changes $(\Delta\vec{X})_i$, $i = 2, 5, 8$ represent death of either a healthy T cell, latently infected T cell or a virion. The change $(\Delta\vec{X})_3 = [-1, 1, 0, -1]^{tr}$ represents a virion that enters a healthy T cell and results in a latently infected cell with probability $pkX_1X_4\Delta t$, and the change $(\Delta\vec{X})_4 = [-1, 0, 1, -1]^{tr}$ results in an actively infected cell with probability $(1-p)kX_1X_4\Delta t$. The change $(\Delta\vec{X})_7 = [0, 0, -1, N]^{tr}$ represents a death of an

actively infected cell and at the same time, the release of $N$ virions. Finally, the change $(\Delta\vec{X})_6$ represents a transition from a latently infected cell to an actively infected cell. An alternate formulation for changes 4 and 5 was considered by Vidurupola [35], where these changes are combined into $[-1, p, 1-p, -1]^{tr}$ with probability $kX_1X_4\Delta t$. Each of the random variables in the expressions for the probabilities are evaluated at time $t$, $X_i = X_i(t)$.

Applying the probabilities in Table 2, the expectation vector and covariance matrix of $\Delta\vec{X}$ are computed. The expectation vector is

$$\mathbb{E}(\Delta\vec{X}) = \sum_{i=1}^{9} p_i(\Delta\vec{X})_i\Delta t = \vec{f}(\vec{X})\Delta t,$$

where

$$\vec{f}(\vec{X}) = \begin{bmatrix} \lambda + rX_1\left(1 - \dfrac{X_{tot}}{T_{\max}}\right) - \mu X_1 - kX_1X_4 \\ pkX_1X_4 - \mu X_2 - \alpha X_2 \\ (1-p)kX_1X_4 + \alpha X_2 - aX_3 \\ NaX_3 - \gamma X_4 - kX_1X_4 \end{bmatrix} \tag{4}$$

is the drift vector. The covariance matrix of $\Delta\vec{X}$ is obtained by dropping the higher-order terms of order $(\Delta t)^2$ or greater,

$$\begin{aligned} \mathbb{E}[(\Delta\vec{X})(\Delta\vec{X})^{tr}] - [\mathbb{E}(\Delta\vec{X})][\mathbb{E}(\Delta\vec{X})]^{tr} &\approx \mathbb{E}((\Delta\vec{X})(\Delta\vec{X})^{tr}) \\ &\approx \sum_{i=1}^{9} p_i(\Delta\vec{X})_i(\Delta\vec{X})_i^{tr}\Delta t \\ &= \Sigma(\vec{X})\Delta t, \end{aligned}$$

where $\Sigma(\vec{X})$ is given by

$$\begin{bmatrix} \varphi + kX_1X_4 & -pkX_1X_4 & -(1-p)kX_1X_4 & kX_1X_4 \\ -pkX_1X_4 & pkX_1X_4 + \mu X_2 + \alpha X_2 & -\alpha X_2 & -pkX_1X_4 \\ -(1-p)kX_1X_4 & -\alpha X_2 & (1-p)kX_1X_4 + \alpha X_2 + aX_3 & -(1-p)kX_1X_4 - NaX_3 \\ kX_1X_4 & -pkX_1X_4 & -(1-p)kX_1X_4 - NaX_3 & kX_1X_4 + N^2aX_3 + \gamma X_4 \end{bmatrix}$$

and $\varphi = \lambda + rX_1\left(1 - \dfrac{X_{tot}}{T_{\max}}\right) + \mu X_1$. A diffusion matrix $G$ satisfies $GG^{tr} = \Sigma$ [2]. One matrix $G$ is

$$\begin{bmatrix} \sqrt{\varphi} & -\sqrt{pkX_1X_4} & -\sqrt{(1-p)kX_1X_4} & 0 & 0 & 0 & 0 \\ 0 & \sqrt{pkX_1X_4} & 0 & -\sqrt{\mu X_2} & -\sqrt{\alpha X_2} & 0 & 0 \\ 0 & 0 & \sqrt{(1-p)kX_1X_4} & 0 & \sqrt{\alpha X_2} & -\sqrt{aX_3} & 0 \\ 0 & -\sqrt{pkX_1X_4} & -\sqrt{(1-p)kX_1X_4} & 0 & 0 & N\sqrt{aX_3} & -\sqrt{\gamma X_4} \end{bmatrix}.$$

The matrix $G$ is not unique; there are other matrices with the property $GG^{tr} = \Sigma$ (see e.g., [2, 8, 17]). Applying the preceding matrix $G$, an Itô system of SDEs is

obtained for the bursting case:

$$
\begin{aligned}
dX_1 &= \left[\lambda + rX_1\left(1-\frac{X_{tot}}{T_{\max}}\right) - \mu X_1 - kX_1X_4\right]dt \\
&\quad + \sqrt{\lambda + rX_1\left(1-\frac{X_{tot}}{T_{\max}}\right) + \mu X_1}dW_1 - \sqrt{pkX_1X_4}dW_2 - \sqrt{(1-p)kX_1X_4}dW_3 \\
dX_2 &= (pkX_1X_4 - \mu X_2 - \alpha X_2)dt + \sqrt{pkX_1X_4}dW_2 - \sqrt{\mu X_2}dW_4 - \sqrt{\alpha X_2}dW_5 \\
dX_3 &= [(1-p)kX_1X_4 + \alpha X_2 - aX_3]dt + \sqrt{(1-p)kX_1X_4}dW_3 \\
&\quad + \sqrt{\alpha X_2}dW_5 - \sqrt{aX_3}dW_6 \\
dX_4 &= (NaX_3 - \gamma X_4 - kX_1X_4)dt - \sqrt{pkX_1X_4}dW_2 - \sqrt{(1-p)kX_1X_4}dW_3 \\
&\quad + N\sqrt{aX_3}dW_6 - \sqrt{\gamma X_4}dW_7,
\end{aligned}
\tag{5}
$$

where $W_i = W_i(t)$, $i = 1, 2, \ldots, 7$ are seven independent Wiener processes.

2.2.2. *Budding.* In the budding case, the virus is produced and released continuously during the life of the infected cells; the virus "buds" from the infected cell. The possible changes are summarized in Table 3.

TABLE 3. Possible state changes in the case of budding during the time interval $\Delta t$, where $X_i = X_i(t)$, $i = 1, 2, 3, 4$.

| $i$ | Change, $(\Delta\vec{X})_i$ | Probability, $p_i\Delta t$ |
|---|---|---|
| 1 | $(\Delta\vec{X})_1 = [1,0,0,0]^{tr}$ | $\left[\lambda + rX_1\left(1-\frac{X_{tot}}{T_{\max}}\right)\right]\Delta t$ |
| 2 | $(\Delta\vec{X})_2 = [-1,0,0,0]^{tr}$ | $\mu X_1\Delta t$ |
| 3 | $(\Delta\vec{X})_3 = [-1,1,0,-1]^{tr}$ | $pkX_1X_4\Delta t$ |
| 4 | $(\Delta\vec{X})_4 = [-1,0,1,-1]^{tr}$ | $(1-p)kX_1X_4\Delta t$ |
| 5 | $(\Delta\vec{X})_5 = [0,-1,0,0]^{tr}$ | $\mu X_2\Delta t$ |
| 6 | $(\Delta\vec{X})_6 = [0,-1,1,0]^{tr}$ | $\alpha X_2\Delta t$ |
| 7 | $(\Delta\vec{X})_7 = [0,0,-1,0]^{tr}$ | $aX_3\Delta t$ |
| 8 | $(\Delta\vec{X})_8 = [0,0,0,1]^{tr}$ | $NaX_3\Delta t$ |
| 9 | $(\Delta\vec{X})_9 = [0,0,0,-1]^{tr}$ | $\gamma X_4\Delta t$ |
| 10 | $(\Delta\vec{X})_{10} = [0,0,0,0]^{tr}$ | $1 - \sum_{i=1}^{9} p_i\Delta t$ |

The only difference between the budding and bursting cases is in the two changes, $(\Delta\vec{X})_7$ and $(\Delta\vec{X})_8$. The assumption in this case is that they are independent. Following a similar procedure as in the bursting case, we find the drift vector and a matrix $H$ such that $HH^{tr} = \tilde{\Sigma}$, where $\tilde{\Sigma}$ is the covariance matrix to order $\Delta t$. The drift vector $\vec{f}$ is the same as for the bursting case. The covariance matrix $\tilde{\Sigma}$ is

$$
\begin{bmatrix}
\varphi + kX_1X_4 & -pkX_1X_4 & -(1-p)kX_1X_4 & kX_1X_4 \\
-pkX_1X_4 & pkX_1X_4 + \mu X_2 + \alpha X_2 & -\alpha X_2 & -pkX_1X_4 \\
-(1-p)kX_1X_4 & -\alpha X_2 & (1-p)kX_1X_4 + \alpha X_2 + aX_3 & -(1-p)kX_1X_4 \\
kX_1X_4 & -pkX_1X_4 & -(1-p)kX_1X_4 & kX_1X_4 + NaX_3 + \gamma X_4
\end{bmatrix},
$$

with $\varphi = \lambda + rX_1\left(1 - \dfrac{X_{tot}}{T_{\max}}\right) + \mu X_1$ and a matrix $H$ is equal to

$$\begin{bmatrix} \sqrt{\varphi} & -\sqrt{pkX_1X_4} & -\sqrt{(1-p)kX_1X_4} & 0 & 0 & 0 & 0 \\ 0 & \sqrt{pkX_1X_4} & 0 & -\sqrt{\mu X_2} & -\sqrt{\alpha X_2} & 0 & 0 \\ 0 & 0 & \sqrt{(1-p)kX_1X_4} & 0 & \sqrt{\alpha X_2} & -\sqrt{aX_3} & 0 \\ 0 & -\sqrt{pkX_1X_4} & -\sqrt{(1-p)kX_1X_4} & 0 & 0 & 0 & \sqrt{NaX_3 + \gamma X_4} \end{bmatrix}.$$

An explicit form for the Itô SDE system in the budding case is

$$\begin{aligned} dX_1 &= \left[\lambda + rX_1\left(1 - \frac{X_{tot}}{T_{\max}}\right) - \mu X_1 - kX_1X_4\right]dt \\ &\quad \sqrt{\lambda + rX_1\left(1 - \frac{X_{tot}}{T_{\max}}\right) + \mu X_1}dW_1 - \sqrt{pkX_1X_4}dW_2 - \sqrt{(1-p)kX_1X_4}dW_3 \\ dX_2 &= (pkX_1X_4 - \mu X_2 - \alpha X_2)dt + \sqrt{pkX_1X_4}dW_2 - \sqrt{\mu X_2}dW_4 - \sqrt{\alpha X_2}dW_5 \\ dX_3 &= [(1-p)kX_1X_4 + \alpha X_2 - aX_3]dt + \sqrt{(1-p)kX_1X_4}dW_3 \\ &\quad + \sqrt{\alpha X_2}dW_5 - \sqrt{aX_3}dW_6 \\ dX_4 &= (NaX_3 - \gamma X_4 - kX_1X_4)dt - \sqrt{pkX_1X_4}dW_2 - \sqrt{(1-p)kX_1X_4}dW_3 \\ &\quad + \sqrt{NaX_3 + \gamma X_4}dW_7, \end{aligned} \tag{6}$$

where $W_i = W_i(t)$, $i = 1, 2, \ldots, 7$ are seven independent Wiener processes.

The two Itô systems of SDEs (5) and (6) differ from the one formulated by Tuckwell and Le Corfec [31]. Tuckwell and Le Corfec include only the variability due to the infection rate caused by collisions and bindings of virus particles to receptors on target cells. The parameter $k$ in the differential equations for $X_i$, $i = 1, 2, 3$ represents the probability per unit time per virion of a collision with and attachment to an uninfected T cell [31]. In the differential equation for $X_4$, the parameter $k$ is the probability per unit time per uninfected T cell of a collision with and attachment to a virion and because the units are different, instead of $k$ another notation such as $k'$ is used. However, the value of the parameter $k = k'$. In our models (5) and (6), the same value for $k$ is applied in all of the differential equations. The SDE model of Tuckwell and Le Corfec has the following form:

$$\begin{aligned} dX_1 &= (\lambda - \mu X_1 - kX_1X_4)dt - \sqrt{kX_1X_4}dW \\ dX_2 &= (pkX_1X_4 - \mu X_2 - \alpha X_2)dt + \sqrt{pkX_1X_4}dW \\ dX_3 &= [(1-p)kX_1X_4 + \alpha X_2 - aX_3]dt + \sqrt{(1-p)kX_1X_4}dW \\ dX_4 &= (NaX_3 - \gamma X_4 - k'X_1X_4)dt - \sqrt{k'X_1X_4}dW. \end{aligned} \tag{7}$$

In system (7), there is only one Wiener process $W = W(t)$.

## 3. Model analysis.

### 3.1. ODE model.

Let the values of $T$, $L$, $I$ and $V$ at the disease-free equilibrium (DFE) be denoted as $\bar{T}$, $\bar{L}$, $\bar{I}$ and $\bar{V}$. Then $\bar{L} = \bar{I} = \bar{V} = 0$. Setting the differential equation for $T$ in (1) to zero, there are two cases for the DFE depending on whether $r > 0$ or $r = 0$. If $r > 0$, then

$$\bar{T} = \frac{(r-\mu) + \sqrt{(r-\mu)^2 + \frac{4r\lambda}{T_{max}}}}{\frac{2r}{T_{max}}}. \tag{8}$$

If $r = 0$, then

$$\bar{T} = \frac{\lambda}{\mu}. \tag{9}$$

In either case, the value of $\bar{T}$ satisfies

$$\frac{\lambda}{\mu} \leq \bar{T} \leq T_{\max}.$$

It is straightforward to obtain conditions for local stability of the DFE. Define the basic reproduction number as

$$\mathcal{R}_0 := \frac{Nk\bar{T}[\alpha p + (1-p)(\mu+\alpha)]}{(\mu+\alpha)(\gamma+k\bar{T})}. \tag{10}$$

If $\mathcal{R}_0 < 1$, then the DFE is locally asymptotically stable and unstable if $\mathcal{R}_0 > 1$. This basic reproduction number differs from the one obtained by the next generation matrix approach [32, 33] but is the one more commonly cited in the literature for special cases of this model [4, 24, 11]. Some alternate thresholds are defined in Appendix A, known as type reproduction numbers when infected cells or the virions are controlled [9, 27]. During the initial stages of the infection, it is often the viral load that is controlled. The value in (10) is the type reproduction for controlling $V$ but we refer to it as the basic reproduction number. The threshold $\mathcal{R}_0 = 1$ defines a critical burst size

$$N_{crit} := \frac{(\mu+\alpha)(\gamma+k\bar{T})}{[\mu(1-p)+\alpha]k\bar{T}}.$$

Setting $p = 1$ leads to the value for $N_{crit}$ given by Perelson et al. [24].

Kamgang and Sallet [11] verified global stability of the DFE in the case $r > 0$ and $p = 1$. We extend the proof to the case $r \geq 0$ and $p \in [0, 1]$ by finding a new Lyapunov function that applies to our system. The value of $T_{max}$ is the maximum number of uninfected T cells in the volume under consideration. If $T(0) \leq \bar{T}$, then it follows from the $T$ equation in (1) that

$$\dot{T} \leq \lambda - \mu T + rT\left(1 - \frac{T}{T_{max}}\right)$$

which implies $T(t) \leq \bar{T}$ because $\bar{T}$ is a unique positive stable equilibrium for the differential equation

$$\dot{x} = \lambda - \mu x + rx\left(1 - \frac{x}{T_{max}}\right).$$

Define the constant $V_0$ and the set $\mathcal{C}$ as follows:

$$V_0 = \max\left\{\frac{Na\bar{T}}{\gamma}, V(0)\right\}$$

and

$$\mathcal{C} = \left\{ (T, L, I, V) \in \mathbb{R}^4_+ | T_{tot} \leq \bar{T}, V \leq V_0 \right\}.$$

The proof of the following theorem is given in Appendix B.

**Theorem 3.1.** *The DFE of model (1) is globally asymptotically stable on the set $\mathcal{C}$ if $\mathcal{R}_0 < 1$ (equivalently if $N < N_{crit}$) and it is unstable if $\mathcal{R}_0 > 1$, where $\bar{T}$ is defined in (8) in the case $r > 0$ and $\bar{T} = \lambda/\mu$ in the case $r = 0$.*

3.2. **SDE models.** The forward Kolmogorov differential equations for the probability density function $P(t,\vec{X})$ can be derived from the drift vector and covariance matrix [3, 22]. For the SDE system in the budding case, model (6), $d\vec{X} = \vec{f}dt + Hd\vec{W}$, where $HH^{tr} = \tilde{\Sigma}$ is the covariance matrix. The density function is a solution of the following partial differential equation:

$$\begin{aligned}
\frac{\partial P(t,\vec{X})}{\partial t} &= \frac{1}{2}\sum_{i=1}^{4}\sum_{j=1}^{4}\frac{\partial^2}{\partial X_i \partial X_j}\left[P(t,\vec{X})\sum_{l=1}^{7}H_{il}H_{jl}\right] - \sum_{i=1}^{4}\frac{\partial[P(t,\vec{X})f_i]}{\partial X_i} \\
&= \frac{1}{2}\Bigg\{\frac{\partial^2}{\partial X_1^2}P(t,\vec{X})\left[\lambda + rX_1\left(1-\frac{X_{tot}}{T_{\max}}\right)+\mu X_1 + kX_1X_4\right] \\
&\quad + \frac{\partial^2}{\partial X_2^2}P(t,\vec{X})\left[pkX_1X_4 + (\mu+\alpha)X_2\right] + \frac{\partial^2}{\partial X_3^2}P(t,\vec{X})\left[(1-p)kX_1X_4 + \alpha X_2 + aX_3\right] \\
&\quad + \frac{\partial^2}{\partial X_4^2}P(t,\vec{X})\left[kX_1X_4 + NaX_3 + \gamma X_4\right]\Bigg\} \\
&\quad - \frac{\partial^2}{\partial X_1\partial X_2}P(t,\vec{X})\left[pkX_1X_4\right] - \frac{\partial^2}{\partial X_1\partial X_3}P(t,\vec{X})\left[(1-p)kX_1X_4\right] \\
&\quad + \frac{\partial^2}{\partial X_1\partial X_4}P(t,\vec{X})\left[kX_1X_4\right] - \frac{\partial^2}{\partial X_2\partial X_3}P(t,\vec{X})\left[\alpha X_2\right] - \frac{\partial^2}{\partial X_2\partial X_4}P(t,\vec{X})\left[pkX_1X_4\right] \\
&\quad - \frac{\partial^2}{\partial X_3\partial X_4}P(t,\vec{X})\left[(1-p)kX_1X_4\right] \\
&\quad - \Bigg\{\frac{\partial}{\partial X_1}P(t,\vec{X})\left[\lambda - \mu X_1 + rX_1\left(1-\frac{X_{tot}}{T_{\max}}\right) - kX_1X_4\right] \\
&\quad + \frac{\partial}{\partial X_2}P(t,\vec{X})[kpX_1X_4 - \mu X_2 - \alpha X_2] + \frac{\partial}{\partial X_3}P(t,\vec{X})[k(1-p)X_1X_4 + \alpha X_2 - aX_3] \\
&\quad + \frac{\partial}{\partial X_4}P(t,\vec{X})[NaX_3 - \gamma X_4 - kX_1X_4]\Bigg\},
\end{aligned}$$

where $f = [f_i]$, $H = [H_{ij}]$ and the expression $\sum_{l=1}^{7} H_{il}H_{jl}$ is the $(i,j)$ element of the $4\times 4$ covariance matrix $\tilde{\Sigma}$. Similar equations can be derived for the bursting case. These equations are too complex to solve directly. Alternatively, to obtain information about the probability density function $P(t,\vec{X})$, the multivariate Itô's formula can be applied to yield SDEs for random functions of the type $X_iX_j$ [1, 3, 22].

The Itô system of SDEs in the budding case has the following form:

$$d\vec{X}(t) = \vec{f}(\vec{X}(t))dt + H(\vec{X}(t))d\vec{W}(t),$$

where $\vec{f} = [f_1, f_2, f_3, f_4]^{tr}$, $H = [H_{ij}]$ is a $4\times 7$ matrix and $\vec{W} = [W_1,\ldots,W_7]^{tr}$. Given the scalar function, $F(t,\vec{X}(t))$, the multivariate Itô's formula can be expressed as

$$dF(t,\vec{X}(t)) = h(t,\vec{X}(t))\,dt + \vec{g}(t,\vec{X}(t))\cdot d\vec{W}(t),$$

such that for $x = [x_1,x_2,x_3,x_4]$,

$$h(t,x) = \frac{\partial F}{\partial t} + \sum_{i=1}^{4}\frac{\partial F}{\partial x_i}f_i + \sum_{i=1}^{4}\sum_{j=1}^{4}\sum_{k=1}^{7}\frac{1}{2}\frac{\partial^2 F}{\partial x_i\partial x_j}H_{ik}H_{jk}$$

and

$$\vec{g}(t,x)\cdot d\vec{W}(t) = \sum_{j=1}^{7}\sum_{i=1}^{4}\frac{\partial F}{\partial x_i}H_{ij}dW_j(t).$$

For models (5) and (6), the second moment of $X_1$ can be computed using $F(t,x) = x_1^2$, $\partial F/\partial t = 0$, $\partial F/\partial x_1 = 2x_1$, $\partial^2 F/\partial x_1^2 = 2$ with the other partial derivatives

equal to zero. Calculating $h$ and $\vec{g}$,

$$\begin{aligned} h(t,\vec{X}(t)) &= 2X_1\left[\lambda-\mu X_1+rX_1\left(1-\frac{X_{tot}}{T_{\max}}\right)-kX_1X_4\right] \\ &\quad+\left[\lambda+\mu X_1+rX_1\left(1-\frac{X_{tot}}{T_{\max}}\right)\right]+kX_1X_4 \end{aligned}$$

and

$$\begin{aligned} \vec{g}\cdot d\vec{W} &= 2X_1\left\{\sqrt{\lambda+\mu X_1+rX_1\left(1-\frac{X_{tot}}{T_{\max}}\right)}dW_1-\sqrt{pkX_1X_4}dW_2\right. \\ &\quad\left.-\sqrt{(1-p)kX_1X_4}dW_3\right\}. \end{aligned}$$

Therefore,

$$\begin{aligned} dX_1^2 &= (2X_1+1)\varphi dt-[(2X_1-1)kX_1X_4+4\mu X_1^2]dt \\ &\quad+2X_1\left\{\sqrt{\varphi}dW_1-\sqrt{pkX_1X_4}dW_2-\sqrt{(1-p)kX_1X_4}dW_3\right\}, \end{aligned}$$

where

$$\varphi=\lambda+rX_1\left(1-\frac{X_{tot}}{T_{\max}}\right)+\mu X_1.$$

The ODEs for the first and second moments for the remaining variables are given in Appendix C.

Applying properties of Itô SDEs and Wiener processes, moment differential equations can be derived. Each moment differential equation depends on higher-order moment equations resulting in an infinite system of differential equations. It is necessary to make some assumptions regarding the higher-order moments to form a finite system of equations. Often a normal or a log-normal assumption is made to "close" the system of differential equations [7, 13, 14, 16, 18, 19, 28]. For example, assuming normality in the variable $X_1$ and in the simple case of no infection, $X_i=0$ for $i=2,3,4$, $X_{tot}=X_1$, then the differential equations for the moments of $X_1$ are the same for the bursting and budding models, systems (5) and (6), respectively. For a normal distribution,

$$\mathbb{E}[X_1^3]=3\mathbb{E}[X_1^2]\mathbb{E}[X_1]-2(\mathbb{E}[X_1])^3.$$

The differential equations for $\mathbb{E}[X_1]$ and $\mathbb{E}[X_1^2]$ are

$$\begin{aligned} \frac{d\mathbb{E}[X_1]}{dt} &= \lambda+(r-\mu)\mathbb{E}[X_1]-\frac{r}{T_{max}}\mathbb{E}[X_1^2] \\ \frac{d\mathbb{E}[X_1^2]}{dt} &= \lambda+(2\lambda+\mu+r)\mathbb{E}[X_1]+\left(2r-2\mu-\frac{r}{T_{\max}}\right)\mathbb{E}[X_1^2] \\ &\quad-\frac{6r}{T_{\max}}\mathbb{E}[X_1]\mathbb{E}[X_1^2]+\frac{4r}{T_{\max}}\mathbb{E}[X_1]^3. \end{aligned} \tag{11}$$

The nonlinear system (11) simplifies to a linear system if $r=0$, with a solution given by

$$\begin{aligned} \mathbb{E}[X_1(t)] &= \frac{\lambda}{\mu}+c_1e^{-\mu t} \\ \mathbb{E}[(X_1(t))^2] &= \frac{\lambda}{\mu}+\frac{\lambda^2}{\mu^2}+c_1\left(\frac{2\lambda}{\mu}+1\right)e^{-\mu t}+c_2e^{-2\mu t}, \end{aligned} \tag{12}$$

where $c_1$ and $c_2$ depend on $\mathbb{E}[X_1(0)]$ and $\mathbb{E}[(X_1(0))^2]$. In the case $r = 0$,

$$\lim_{t\to\infty} \mathbb{E}[X_1(t)] = \frac{\lambda}{\mu} = \lim_{t\to\infty} \mathbb{V}ar[X_1(t)];$$

the mean and variance approach the DFE. For model (7), if $X_4 = 0$, the equation for $X_1$ is an ODE, so that no assumptions are needed to close the system. In this case, the solution for $X_1$ is given by the mean (12) and $\mathbb{V}ar[X_1(t)] = 0$.

4. **Numerical examples.** We illustrate some of the dynamics of the SDE models and compare them with the ODE model. We use two sets of parameter values for our numerical simulations that have been applied to HIV-1. For the model with $r = 0$, we use parameter values given in Tuckwell and Le Corfec [31], Table 4, but with different initial conditions. The basic reproduction number for the ODE model is $\mathcal{R}_0 = 7.9$ with critical burst size $N_{crit} = 38$. For the model with $r > 0$, we use the parameter values given in Perelson et al. [24], Table 5, for the slow/low strain of HIV-1 that is able to evade the immune response, with the exception that we let parameter $p = 0.1$. Perelson et al. assume all infected target cells are latent prior to becoming actively infected, $p = 1$. The basic reproduction number for the ODE model in this case is $\mathcal{R}_0 = 2.7$ with critical burst size $N_{crit} = 111$. We let the total volume be denoted as $v$ mm$^3$ which may depend on whether studies are *in vitro* or *in vivo* and on the particular animal model. In the references, it was assumed that the blood volume in humans is approximately $v = 5 \times 10^6$ mm$^3$. In the parameter set in Table 4, only a proportion of the initial healthy T cells are activated, $T(0) = 200v$. In the parameter set in Table 5, $T(0) = 1000v$. The initial number of virions is a fixed number, independent of $v$.

TABLE 4. Parameter values and initial conditions for $r = 0$. The basic reproduction number is $\mathcal{R}_0 = 7.9$ and critical burst size is $N_{crit} = 38$ [31].

| Parameter | Value | Initial Values |
|---|---|---|
| $\lambda$ | $0.272v$ cells/(day $v$ mm$^3$) | $T(0) = 200v/(v$ mm$^3)$ |
| $\mu$ | 0.00136/day | $L(0) = 0v/(v$ mm$^3)$ |
| $a$ | 0.035/day | $I(0) = 0v/(v$ mm$^3)$ |
| $\gamma$ | 2/day | $V(0) = 10/(v$ mm$^3)$ |
| $k$ | $2.7\times10^{-4}v$ mm$^3$/($v$ [virions or cells] day) | |
| $\alpha$ | $3.6\times10^{-2}$/day | |
| $N$ | 300 virions/cell | |
| $p$ | 0.1 | |

Figure 2 compares the ODE solution with a sample path and stochastic mean of the SDE models (based on 10,000 sample paths) when $r = 0$, the bursting model (5). In Figure 2 (a) the volume is $v = 1$ mm$^3$, in Figure 2 (b) $v = 1000$ mm$^3$ and in Figure 2 (c), $v = 5 \times 10^6$ mm$^3$. A locally stable endemic equilibrium exists for the ODE model since $\mathcal{R}_0 = 7.9 > 1$. The stable equilibrium is $(\hat{T}, \hat{L}, \hat{I}, \hat{V}) = (25, 0.64, 6.8, 35)v$. The total number of T cells at equilibrium is $(25+0.64+6.8)v \approx 32.5v < \bar{T} = 200v$. The total T cell population is depleted, as demonstrated by Phillips [26]. The stochastic mean is calculated based on 10,000 sample paths of the

TABLE 5. Parameter values and initial conditions for $r = 0.03$. The basic reproduction number is $\mathcal{R}_0 = 2.7$ and critical burst size is $N_{crit} = 111$. (*Perelson et al. [24], $p = 1$)

| Parameter | Value | Initial Values |
|---|---|---|
| $\lambda$ | $10v$ cells/(day $v$ mm$^3$) | $T(0) = 1000v/(v$ mm$^3)$ |
| $\mu$ | 0.02/day | $L(0) = 0v/(v$ mm$^3)$ |
| $a$ | 0.24/day | $I(0) = 0v/(v$ mm$^3)$ |
| $\gamma$ | 2.4/day | $V(0) = 50/(v$ mm$^3)$ |
| $k$ | $2.4\times10^{-5}v$ mm$^3$/($v$ [virions or cells] day) | |
| $\alpha$ | $3\times10^{-3}$/day | |
| $N$ | 300 virions/cell | |
| $p$ | 0.1* | |
| $T_{max}$ | $1500v/(v$ mm$^3)$ | |

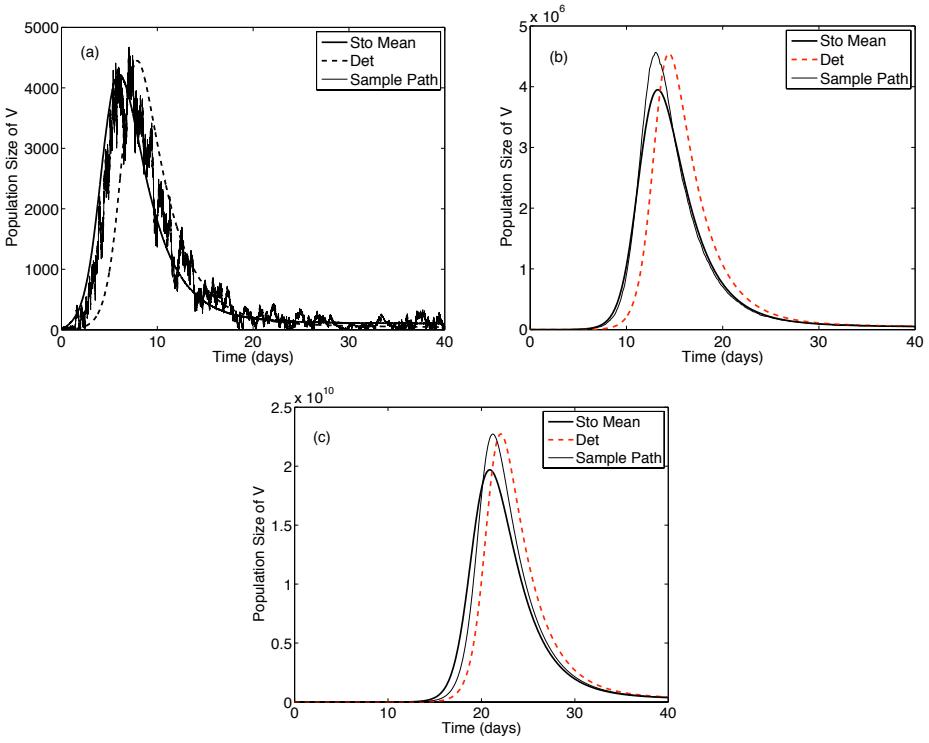


FIGURE 2. ODE solution (Det=dashed curve), one SDE sample path (thin curve) and stochastic mean (Sto Mean=thick curve, calculated from 10,000 sample paths) for free virions in the bursting model (5) with parameter values in Table 4 and $r = 0$. (a) $v = 1$ mm$^3$; (b) $v = 1000$ mm$^3$; (c) $v = 5 \times 10^6$ mm$^3$.

SDE models. The Euler-Maruyama method is used to numerically solve the SDE models.

There is a small probability of viral extinction in the SDE models but it is close to zero because the initial viral load although small is sufficiently large with $\mathcal{R}_0 > 1$ to ensure the virus becomes established. The standard deviation relative to the mean becomes relatively small when the volume is large so that the variability in the sample paths is not visible in Figure 2 (b) and (c). Also, the time to reach the viral peak depends on initial viral concentration and release strategy. The peak is reached earlier with a larger initial viral concentration (compare (a), (b) and (c) in Figure 2). In addition, the variability in the time to reach the peak in the budding model is greater than in the bursting model (compare (a), (b) and (c) in Figure 3).

The variability in the peak viral load was also observed in the SDE model of Tuckwell and Le Corfec [31], model (7). Based on 100 sample paths, 95% confidence intervals were computed for the mean time of the maximum viral peak in models (5), (6) and (7) for parameter values in Table 4 for $v = 5\times10^6$ mm$^3$. The time of the maximum viral peak in the ODE model is at 21.04 days, whereas for the bursting model, the 95% confidence interval (CI) for the mean time of the viral peak is $[19.02, 19.26]$, for budding the 95% CI is $[20.44, 21.05]$ and for model (7) the 95% CI is $[20.34, 20.72]$. The mean time of the viral peak in the budding model cannot be distinguished from the ODE model. The mean peak viral load is significantly earlier in the bursting model and in model (7) than in the ODE model.

The early viral peak is also visible in the bursting model for parameter values from Table 5 with $r = 0.03$. The DFE for the ODE model is $\bar{T} = 1435v$ and the stable endemic equilibrium is $(\hat{T}, \hat{L}, \hat{I}, \hat{V}) = (366, 45, 39, 1178)v$. Six sample paths for the bursting and budding models with $v = 5 \times 10^6$ mm$^3$ are graphed in Figure 4. The time of the maximum viral peak in the ODE model is 73.3 days. From 100 sample paths, the 95% CI for the mean time of the viral peak for bursting is $[67.5, 68.3]$ and for budding the 95% CI is $[74.0, 77.1]$.

One final numerical example illustrates the approximate quasistationary distribution (conditioned on nonextinction) for the healthy T cells and free virions and the formulas for the moments derived from multivariate Itô's formula. For the budding model (6) with parameter values from Table 5, $v = 100$ mm$^3$ and $r = 0.03$ by the time $t = 400$ days, the stable equilibrium is reached in the ODE model, $(\hat{T}, \hat{L}, \hat{I}, \hat{V}) = (366, 45, 39, 1178)v$. Probability histograms for the healthy T-cell population and free virions are computed at $t = 400$ based on 10,000 sample paths and graphed in Figure 5. The mean $\hat{\mu}_i$ and standard deviation $\hat{\sigma}_i$, $i = T, V$, estimated from the sample paths were used to fit to a normal distribution

$$\hat{\mu}_T = 36,700, \quad \hat{\sigma}_T = 554, \quad \hat{\mu}_V = 117,000, \quad \hat{\sigma}_T = 5020. \tag{13}$$

The equilibrium values for the first and second moments under the assumption of normality were computed from the differential equations given in Appendix C. The equilibrium values for the mean and standard deviation of $X_1$ and $X_4$, corresponding to the random variables $T$ and $V$, respectively, are

$$\mathbb{E}(X_1) = 36,650, \quad \sqrt{\mathbb{V}ar(X_1)} = 561, \quad \mathbb{E}(X_4) = 117,800, \quad \sqrt{\mathbb{V}ar(X_4)} = 4987.$$

There is good agreement with the estimates from the simulations, given in equation (13). For larger volumes, the means are approximately proportional to $v$, whereas the standard deviations are approximately proportional to $\sqrt{v}$.

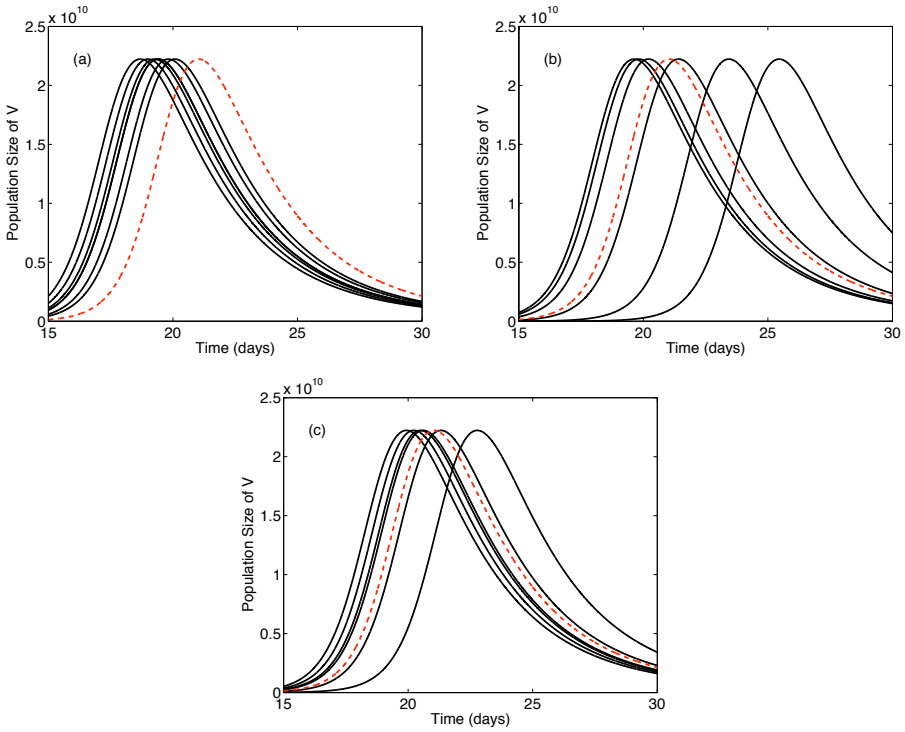


FIGURE 3. ODE solution (dashed curve) and six SDE sample paths (solid curves) for free virions for parameter values in Table 4, $v = 5 \times 10^6$ mm$^3$ and $r = 0.$; (a) bursting model (5); (b) budding model (6); (c) Tuckwell and Le Corfec model (7).

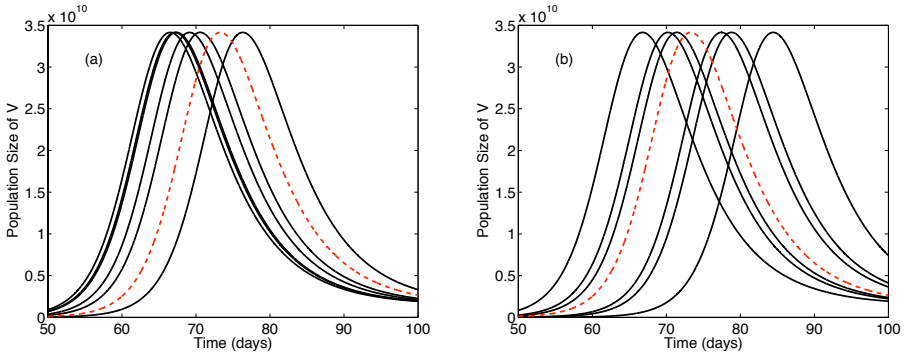


FIGURE 4. ODE solution (dashed curve) and six SDE sample paths (solid curves) for parameter values given in Table 5, $v = 5 \times 10^6$ mm$^3$ and $r = 0.03$; (a) bursting model (5); (b) budding model (6).

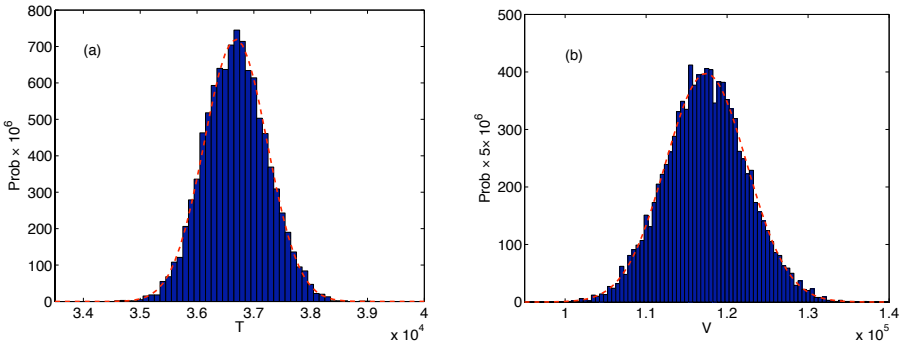


FIGURE 5. Probability histograms based on 10,000 sample paths at $t = 400$ days for the budding model (6) for parameter values in Table 5, $v = 100$ mm$^3$ and $r = 0.03$; (a) healthy T cell population, $\hat{\mu}_T = 36,700$, $\hat{\sigma}_T = 554$; (b) free virions, $\hat{\mu}_V = 117,000$, $\hat{\sigma}_V = 5020$. The normal approximation is the dashed curve.

5. **Discussion.** A basic virus-cell ODE model with healthy target cells, latent and actively infected target cells and free virions is used to derive two new Itô SDE models. Although the ODE model was originally applied to HIV-1 [24, 26], the simplicity of the model allows it to be applied to other intra-host viral infections during the early stages of infection. The new Itô SDEs are distinguished by the method which the virus is released from the host cell, either budding or bursting. Bursting assumes the infected host cell dies at the same time $N$ (burst size) virions are released, whereas in budding, virions are continuously released during the life of an actively infected cell. Many types of viruses use one or both of these release strategies. The distinction between budding and bursting is usually associated with the presence or the absence of a viral envelope, but this is not always the case [6].

The Itô SDE models for virus-cell interactions incorporate more realism into the mechanisms for viral entry and release than the ODE models and show distinct differences from the ODE model. The variability in the SDE models depends on the concentration, with much greater variability for small concentrations than large concentrations (see e.g., [17]). The SDE models also show a large variability in the timing of the viral peak (especially for the budding model) and a significantly earlier mean time for the viral peak (with bursting), which may have implications for viral evolution. From the viewpoint of the virus, there is an advantage to early establishment. It has been shown, prior to activation of the immune system, that bursting is a more successful strategy than budding, i.e., the probability of viral extinction is smaller for bursting than budding [15, 23, 37].

**Appendix** A. **Alternate thresholds.** Alternate expressions for a threshold reproduction number can be computed via the next generation approach and via a type reproduction number. These other thresholds are equivalent to $\mathcal{R}_0 \leq 1$, where $\mathcal{R}_0$ is defined in (10).

In the next generation matrix approach [32, 33], the vectors $\mathcal{F}$ and $\mathcal{V}$ are computed, representing inflow and outflow from disease compartments $L$, $I$ and $V$.

That is,

$$\begin{aligned}\begin{bmatrix}\dot{L}\\ \dot{I}\\ \dot{V}\end{bmatrix} &= \begin{bmatrix}kpTV\\ k(1-p)TV\\ NaI\end{bmatrix} - \begin{bmatrix}\mu L+\alpha L\\ -\alpha L+aI\\ \gamma V+kTV\end{bmatrix}\\ &= \mathcal{F}-\mathcal{V}\\ &\approx (F-V)\begin{bmatrix}L\\ I\\ V\end{bmatrix},\end{aligned}$$

where

$$F=\begin{bmatrix}0 & 0 & kp\bar{T}\\ 0 & 0 & k(1-p)\bar{T}\\ 0 & Na & 0\end{bmatrix}$$

and

$$V=\begin{bmatrix}\mu+\alpha & 0 & 0\\ -\alpha & a & 0\\ 0 & 0 & \gamma+k\bar{T}\end{bmatrix}.$$

Then the next generation matrix $K=FV^{-1}$ is

$$K=\begin{bmatrix}0 & 0 & \dfrac{kp\bar{T}}{\gamma+k\bar{T}}\\ 0 & 0 & \dfrac{k(1-p)\bar{T}}{\gamma+k\bar{T}}\\ \dfrac{N\alpha}{\mu+\alpha} & N & 0\end{bmatrix}. \tag{14}$$

The basic reproduction number is defined as the spectral radius of $K$:

$$\rho(K)=\sqrt{\frac{Nk\bar{T}[\alpha p+(1-p)(\mu+\alpha)]}{(\mu+\alpha)(\gamma+k\bar{T})}}=\sqrt{\mathcal{R}_0}.$$

The type reproduction number is another threshold value proposed by Roberts and Heesterbeek [9, 27]. The type reproduction applies the next generation matrix but it singles out particular types of hosts. The value of the type reproduction gives an indication of the effort required to control the particular type.

Suppose the goal is to control the virus population, then the type reproduction corresponding to $V$ is defined as follows:

$$T_v=e_v^{tr}K(\mathbb{I}-(\mathbb{I}-P_v)K)^{-1}e_v,$$

where $e_v=[0,0,1]^{tr}$,

$$P_v=\begin{bmatrix}0 & 0 & 0\\ 0 & 0 & 0\\ 0 & 0 & 1\end{bmatrix},$$

$\mathbb{I}$ is the identity matrix and $K$ is the next generation matrix given in (14). Since $\rho((\mathbb{I}-P_v)K)=0$, the inverse is well defined. Hence,

$$T_v=\frac{k\bar{T}N[\alpha p+(1-p)(\mu+\alpha)]}{(\mu+\alpha)(\gamma+k\bar{T})}=\mathcal{R}_0,$$

where $\mathcal{R}_0$ as defined in (10).

If the goal is to control the infected T cells, then the type reproduction number corresponding to $I$ is

$$T_i=e_i^{tr}K(\mathbb{I}-(\mathbb{I}-P_i)K)^{-1}e_i,$$

where $e_i = [0,1,0]^{tr}$,

$$P_i = \begin{bmatrix} 0 & 0 & 0 \\ 0 & 1 & 0 \\ 0 & 0 & 0 \end{bmatrix}.$$

Then

$$T_i = \frac{k\bar{T}N(1-p)}{(\gamma + k\bar{T})\left(1 - \dfrac{pk\bar{T}N\alpha}{(\mu+\alpha)(\gamma+k\bar{T})}\right)}.$$

An additional assumption is required so that the inverse exists:

$$\frac{pk\bar{T}N\alpha}{(\mu+\alpha)(\gamma+k\bar{T})} < 1. \tag{15}$$

Thus, inequality (15) and $T_i < 1$ if and only if $\mathcal{R}_0 < 1$.

If the goal is to control latently infected cells, then the type reproduction for $L$ is

$$T_l = \frac{(1-p)k\bar{T}N\alpha}{(\mu+\alpha)(\gamma+k\bar{T})\left(1 - \dfrac{(1-p)k\bar{T}N}{\gamma+k\bar{T}}\right)}$$

provided

$$\frac{(1-p)k\bar{T}N}{\gamma+k\bar{T}} < 1. \tag{16}$$

Thus, inequality (16) and $T_l < 1$ if and only if $\mathcal{R}_0 < 1$. If all infected cells and virions are to be controlled, then the type reproduction number equals the basic reproduction number as computed via the next generation matrix approach, $T_{l,i,v} = \rho(K)$.

**Appendix** B. **Proof of theorem.** First, we define a compact positively invariant subset $\mathcal{C} \subset \mathbb{R}^4_+$ for system (1) when $r \geq 0$, where $\mathbb{R}^4_+ = \{\mathbf{x} | \mathbf{x} = (x_1, x_2, x_3, x_4) \in \mathbb{R}^4, x_i \geq 0, i = 1,2,3,4\}$. Note that

$$\left.\frac{dT}{dt}\right|_{T=0} = \lambda > 0, \quad \left.\frac{dL}{dt}\right|_{L=0} = kpTV \geq 0$$

$$\left.\frac{dI}{dt}\right|_{I=0} = k(1-p)TV + \alpha L \geq 0, \quad \left.\frac{dV}{dt}\right|_{V=0} = NaI \geq 0.$$

As already shown $T(t) \leq \bar{T}$ if $T(0) \leq \bar{T}$. The presence of infection decreases the healthy T cell population. We prove $T_{tot}(t) = T(t) + L(t) + I(t) \leq \bar{T}$, if $T_{tot}(0) \leq \bar{T}$. If $T(0) > 0$ and $V(0) > 0$, then it can be shown that solutions to (1) are positive for $t > 0$. From (1), it follows that

$$\frac{dT_{tot}}{dt} = \lambda - \mu T_{tot} - (a-\mu)I + rT\left(1 - \frac{T_{tot}}{T_{max}}\right).$$

Since $a > \mu$ (assumption (2)) and $I(t) \geq 0$ it follows that

$$\frac{dT_{tot}}{dt} \leq \lambda - \mu T_{tot} + rT\left(1 - \frac{T_{tot}}{T_{max}}\right). \tag{17}$$

Suppose $\tilde{t}$ is the first time $T_{tot}(\tilde{t}) = \bar{T}$. Using the facts that $\bar{T} < T_{\max}$ and $T(t) < T_{tot}(t)$ for $t > 0$, then at $t = \tilde{t}$, the right side of (17) is negative,

$$\left.\frac{dT_{tot}}{dt}\right|_{T_{tot}=\bar{T}} < \lambda - \mu T_{tot} + rT_{tot}\left(1 - \frac{T_{tot}}{T_{max}}\right)\Bigg|_{T_{tot}=\bar{T}} = 0$$

because $\bar{T}$ is a zero of the right side of the preceding expression. With infection, the total T cell population, $T_{tot}$, is bounded above by $\bar{T}$. Because $T_{tot}(t) \leq \bar{T}$, then $\dot{V} \leq Na\bar{T} - \gamma V$ which implies

$$V(t) \leq \max\left\{\frac{Na\bar{T}}{\gamma}, V(0)\right\} = V_0.$$

The set

$$\mathcal{C} = \left\{ (T, L, I, V) \in \mathbb{R}^4_+ | T_{tot} \leq \bar{T}, V \leq V_0 \right\}$$

is positively invariant. We construct a Lyapunov function to show that the system is globally asymptotically stable if $\mathcal{R}_0 < 1$.

Define $\mathcal{L}$ as follows:

$$\mathcal{L}(T, L, I, V) = [(\gamma + k\bar{T}) - k\bar{T}N(1-p)]L + pk\bar{T}NI + pk\bar{T}V.$$

If $\mathcal{R}_0 < 1$, then

$$\frac{Nk\bar{T}(1-p)}{\gamma + k\bar{T}} < \mathcal{R}_0 < 1.$$

This implies $\mathcal{L}(T, L, I, V) \geq 0$ and $\mathcal{L}(T, L, I, V) = 0$ only if $I = L = V = 0$. Taking the derivative of $\mathcal{L}$ along solution trajectories gives

$$\begin{aligned}
\dot{\mathcal{L}}(T, L, I, V) &= [(\gamma + k\bar{T}) - k\bar{T}N(1-p)]\dot{L} + pk\bar{T}N\dot{I} + pk\bar{T}\dot{V} \\
&= [(\gamma + k\bar{T}) - k\bar{T}N(1-p)][kpTV - \mu L - \alpha L] \\
&\quad + pk\bar{T}N[k(1-p)TV + \alpha L - aI] + pk\bar{T}[NaI - \gamma V - kTV] \\
&= \underbrace{\{Nk\bar{T}[\mu(1-p) + \alpha] - (\mu + \alpha)(\gamma + k\bar{T})\}}_{<0} L - pk\gamma \underbrace{(\bar{T} - T)}_{\geq 0} V
\end{aligned}$$

Therefore, $\dot{\mathcal{L}}(T, L, I, V) \leq 0$.

To show that the DFE is globally asymptotically stable by Lyapunov's direct method, it is necessary to show that the only set where $\dot{\mathcal{L}}(T, L, I, V) = 0$ is the set consisting of only a single point, the DFE [34].

Consider $E = \{\mathbf{x} \in \mathcal{C} | \dot{\mathcal{L}}(\mathbf{x}) = 0\}$ and let $\mathcal{S}$ be the largest invariant set contained in $E$. For $\mathbf{x} \in \mathcal{S}$, we must have $L = 0$ and either $T = \bar{T}$ or $V = 0$. If $L = 0$ and $V = 0$, it follows from the system (1) that $I = 0$, which in turn implies $T = \bar{T}$. If $L = 0$ and $T = \bar{T}$, then $I = 0 = V$. Thus, in both cases, the largest invariant set $\mathcal{S}$ consists of only the point $(\bar{T}, 0, 0, 0)$, the DFE. This proves the global asymptotic stability of the DFE.

A formula for an endemic equilibrium in $\mathcal{C}$ is:

$$T^* = \frac{\gamma(\mu + \alpha)}{kA}, \quad L^* = \frac{\gamma p V^*}{A}, \quad I^* = \frac{\gamma V^*(\alpha + (1-p)\mu)}{aA}$$

where $A = \mu N(1-p) + \alpha N - \mu - \alpha > 0$ since $N > N_{crit}$. It is easy to see that $T^* > 0$ and $L^*, I^* > 0$ if $V^* > 0$. Next the value of $V^*$ is

$$V^* = \frac{\lambda + (r - \mu)T^* - rT^*(T^* + L^* + I^*)/T_{\max}}{kT^*}.$$

As shown in the preceding arguments, an endemic equilibrium in $\mathcal{C}$ must satisfy $T^* + L^* + I^* < \bar{T} < T_{\max}$. For $r = 0$,

$$V^* > \frac{\mu}{kT^*}\left(\frac{\lambda}{\mu} - T^*\right) > 0$$

since $T^* < \lambda/\mu$ at an endemic equilibrium. For $r > 0$, this endemic equilibrium is computed based on the given parameter values.

**Appendix** C. **Moment differential equations in the budding case.** Differential equations for the higher-order moments are given below.

$$
\begin{aligned}
\frac{d\mathbb{E}[X_1]}{dt} &= \lambda + (r-\mu)\mathbb{E}[X_1] - \frac{r}{T_{max}}\left\{\mathbb{E}[X_1^2] + \mathbb{E}[X_1X_2] + \mathbb{E}[X_1X_3]\right\} - k\mathbb{E}[X_1X_4] \\
\frac{d\mathbb{E}[X_2]}{dt} &= kp\mathbb{E}[X_1X_4] - \mu\mathbb{E}[X_2] - \alpha\mathbb{E}[X_2] \\
\frac{d\mathbb{E}[X_3]}{dt} &= k(1-p)\mathbb{E}[X_1X_4] + \alpha\mathbb{E}[X_2] - a\mathbb{E}[X_3] \\
\frac{d\mathbb{E}[X_4]}{dt} &= Na\mathbb{E}[X_3] - \gamma\mathbb{E}[X_4] - k\mathbb{E}[X_1X_4] \\
\frac{d\mathbb{E}[X_1^2]}{dt} &= \lambda + (2\lambda+\mu+r)\mathbb{E}[X_1] - \frac{r}{T_{\max}}\mathbb{E}[X_1X_2] - \frac{r}{T_{\max}}\mathbb{E}[X_1X_3] + k\mathbb{E}[X_1X_4] \\
&\quad + \left(2r - 2\mu - \frac{r}{T_{\max}}\right)\mathbb{E}[X_1^2] - \frac{2r}{T_{\max}}\mathbb{E}[X_1^3] - \frac{2r}{T_{\max}}\mathbb{E}[X_1^2X_2] \\
&\quad - \frac{2r}{T_{\max}}\mathbb{E}[X_1^2X_3] - 2k\mathbb{E}[X_1^2X_4] \\
\frac{d\mathbb{E}[X_2^2]}{dt} &= 2kp\mathbb{E}[X_1X_2X_4] - 2\mu\mathbb{E}[X_2^2] - 2\alpha\mathbb{E}[X_2^2] + pk\mathbb{E}[X_1X_4] + \mu\mathbb{E}[X_2] + \alpha\mathbb{E}[X_2] \\
\frac{d\mathbb{E}[X_3^2]}{dt} &= 2k(1-p)\mathbb{E}[X_1X_3X_4] + 2\alpha\mathbb{E}[X_2X_3] - 2a\mathbb{E}[X_3^2] + (1-p)k\mathbb{E}[X_1X_4] \\
&\quad + \alpha\mathbb{E}[X_2] + a\mathbb{E}[X_3] \\
\frac{d\mathbb{E}[X_4^2]}{dt} &= 2Na\mathbb{E}[X_3X_4] - 2\gamma\mathbb{E}[X_4^2] - 2k\mathbb{E}[X_1X_4^2] + pk\mathbb{E}[X_1X_4] + Na\mathbb{E}[X_3] \\
&\quad + \gamma\mathbb{E}[X_4] + (1-p)k\mathbb{E}[X_1X_4] \\
\frac{d\mathbb{E}[X_1X_2]}{dt} &= \lambda\mathbb{E}[X_2] + (r-2\mu-\alpha)\mathbb{E}[X_1X_2] - pk\mathbb{E}[X_1X_4] - \frac{r}{T_{\max}}\mathbb{E}[X_1X_2X_3] \\
&\quad - k\mathbb{E}[X_1X_2X_4] - \frac{r}{T_{\max}}\left\{\mathbb{E}[X_1^2X_2] + \mathbb{E}[X_1X_2^2]\right\} + kp\mathbb{E}[X_1^2X_4] \\
\frac{d\mathbb{E}[X_1X_3]}{dt} &= \lambda\mathbb{E}[X_3] + (r-\mu-a)\mathbb{E}[X_1X_3] - k(1-p)\left\{\mathbb{E}[X_1X_4] - \mathbb{E}[X_1^2X_4]\right\} \\
&\quad + \alpha\mathbb{E}[X_1X_2] - k\mathbb{E}[X_1X_3X_4] \\
&\quad - \frac{r}{T_{\max}}\left\{\mathbb{E}[X_1X_2X_3] + \mathbb{E}[X_1^2X_3] + \mathbb{E}[X_1X_3^2]\right\} \\
\frac{d\mathbb{E}[X_1X_4]}{dt} &= \lambda\mathbb{E}[X_4] + (r-\mu+k-\gamma)\mathbb{E}[X_1X_4] + Na\mathbb{E}[X_1X_3] - \frac{r}{T_{\max}}\mathbb{E}[X_1X_2X_4] \\
&\quad - \frac{r}{T_{\max}}\mathbb{E}[X_1X_3X_4] - \left(\frac{r}{T_{\max}} + k\right)\mathbb{E}[X_1^2X_4] - k\mathbb{E}[X_1X_4^2] \\
\frac{d\mathbb{E}[X_2X_3]}{dt} &= kp\mathbb{E}[X_1X_3X_4] - \mu\mathbb{E}[X_2X_3] - \alpha\mathbb{E}[X_2X_3] + k(1-p)\mathbb{E}[X_1X_2X_4] \\
&\quad + \alpha\mathbb{E}[X_2^2] - a\mathbb{E}[X_2X_3] - \alpha\mathbb{E}[X_2] \\
\frac{d\mathbb{E}[X_2X_4]}{dt} &= kp\mathbb{E}[X_1X_4^2] - \mu\mathbb{E}[X_2X_4] - \alpha\mathbb{E}[X_2X_4] + Na\mathbb{E}[X_2X_3] - \gamma\mathbb{E}[X_2X_4] \\
&\quad - k\mathbb{E}[X_1X_2X_4] - pk\mathbb{E}[X_1X_4] \\
\frac{d\mathbb{E}[X_3X_4]}{dt} &= k(1-p)\mathbb{E}[X_1X_4^2] + \alpha\mathbb{E}[X_2X_4] - a\mathbb{E}[X_3X_4] + Na\mathbb{E}[X_3^2] - \gamma\mathbb{E}[X_3X_4] \\
&\quad - k\mathbb{E}[X_1X_3X_4] - (1-p)k\mathbb{E}[X_1X_4].
\end{aligned}
$$

From the normality assumption, third moments in the above system can be replaced by lower moments as follows:

$$\begin{aligned}
\mathbb{E}[X_1^3] &= 3\mathbb{E}[X_1^2]\mathbb{E}[X_1] - 2(\mathbb{E}[X_1])^3 \\
\mathbb{E}[X_1^2X_2] &= 2\mathbb{E}[X_1]\mathbb{E}[X_1X_2] + \mathbb{E}[X_1^2]\mathbb{E}[X_2] - 2(\mathbb{E}[X_1])^2\mathbb{E}[X_2] \\
\mathbb{E}[X_1X_2^2] &= 2\mathbb{E}[X_2]\mathbb{E}[X_1X_2] + \mathbb{E}[X_1]\mathbb{E}[X_2^2] - 2\mathbb{E}[X_1](\mathbb{E}[X_2])^2 \\
\mathbb{E}[X_1X_2X_3] &= \mathbb{E}[X_1]\mathbb{E}[X_2X_3] + \mathbb{E}[X_2]\mathbb{E}[X_1X_3] + \mathbb{E}[X_3]\mathbb{E}[X_1X_2] \\
&\quad -2\mathbb{E}[X_1]\mathbb{E}[X_2]\mathbb{E}[X_3].
\end{aligned}$$

The resulting finite system of moment equations can be solved for the first and second moments using a computer algebra system such as Maple. We solved the system of 14 equations for a stable equilibrium solution for parameter values in Table 5 with $r = 0.03$ and $v = 100$ mm$^3$. The following stable equilibrium solution was obtained, $\mathbb{E}[X_1] = 36650$, $\mathbb{E}[X_2] = 4504$, $\mathbb{E}[X_3] = 3941$, $\mathbb{E}[X_4] = 117800$, $\mathbb{E}[X_1^2] = 1.344\times10^9$, $\mathbb{E}[X_2^2] = 2.029\times10^7$, $\mathbb{E}[X_3^2] = 1.556\times10^7$, $\mathbb{E}[X_4^2] = 1.390\times10^{10}$, $\mathbb{E}[X_1X_2] = 1.651\times10^8$, $\mathbb{E}[X_1X_3] = 1.444\times10^8$, $\mathbb{E}[X_1X_4] = 4.316\times10^9$, $\mathbb{E}[X_2X_3] = 1.775\times10^7$, $\mathbb{E}[X_2X_4] = 5.307\times10^8$, $\mathbb{E}[X_3X_4] = 4.651\times10^8$. It should be noted that there exist other equilibria but they are not necessarily stable. The eigenvalues of the $14\times14$ Jacobian matrix evaluated at this equilibrium have negative real part: $-0.0344\pm0.155i$, $-0.0172\pm0.0773i$, $-0.0411\pm0.0773i$, $-2.665\pm0.0776i$, $-0.0239$, $-0.0344$, $-0.0478$, $-2.646$, $-2.674$, $-5.296$.

## REFERENCES


[1] E. Allen, "Modeling with Itô Stochastic Differential Equations," Springer, Dordrecht, The Netherlands, 2007.

[2] E. J. Allen, L. J. S. Allen, A. Arciniega and P. E. Greenwood, *Construction of equivalent stochastic differential equation models*, Stochastic Analysis and Applications, **26** (2008), 274–297.

[3] L. J. S. Allen, "An Introduction to Stochastic Processes with Applications to Biology," $2^{nd}$ edition, Chapman Hall/CRC Press, Boca Raton, FL, 2010.

[4] D. Burg, L. Rong, A. U. Neumann and H. Dahari, *Mathematical modeling of viral kinetics under immune control during primary HIV-1 infection*, Journal of Theoretical Biology, **259** (2009), 751–759.

[5] D. Chao, M. Davenport, S. Forrest and A. Perelson, *A stochastic model of cytotoxic T cell responses*, Journal of Theoretical Biology, **228** (2004), 227–240.

[6] E. T. Clayson, L. V. Jones Brando and R. W. Compans, *Release of simian virus 40 virions from epithelial cells is polarized and occurs without cell lysis*, Journal of Virology, **63** (1989), 2278–2288.

[7] A. J. Ekanayake and L. J. S. Allen, *Comparison of Markov chain and stochastic differential equation population models under higher-order moment closure approximations*, Stochastic Analysis and Applications, **28** (2010), 907–927.

[8] D. T. Gillespie, *The chemical Langevin equation*, The Journal of Chemical Physics, **113** (2000), 297–306.

[9] J. Heesterbeek and M. G. Roberts, *The type-reproduction number T in models for infectious disease control*, Mathematical Biosciences, **206** (2007), 3–10.

[10] C. B. Jonsson, L. T. M. Figueiredo and O. Vapalahti, *A global perspective on hantavirus ecology, epidemiology, and disease*, Clinical Microbiology Reviews, **23** (2010), 412–441.

[11] J. C. Kamgang and G. Sallet, *Computation of threshold conditions for epidemiological models and global stability of the disease-free equilibrium (DFE)*, Mathematical Biosciences, **213** (2008), 1–12.

[12] H. Kamina, R. Makuch and H. Zhao, *A stochastic modeling of early HIV-1 population dynamics*, Mathematical Biosciences, **170** (2001), 187–198.

[13] M. J. Keeling, *Metapopulation moments: Coupling, stochasticity and persistence*, Journal of Animal Ecology, **69** (2000), 725–736.

[14] M. J. Keeling, *Multiplicative moments and measure of persistence in ecology*, Journal of Theoretical Biology, **205** (2000), 269–281.
[15] N. L. Komarova, *Viral reproductive strategies: How can lytic viruses be evolutionarily competitive?*, Journal of Theoretical Biology, **249** (2007), 766–784.
[16] I. Krishnarajah, A. Cook, G. Marion and G. Gibson, *Novel moment closure approximations in stochastic epidemics*, Bulletin of Mathematical Biology, **67** (2005), 855–873.
[17] T. G. Kurtz, *Strong approximation theorems for density dependent Markov chains*, Stochastic Processes and their Applications, **6** (1978), 223–240.
[18] A. L. Lloyd, *Estimating variability in models for recurrent epidemics: Assessing the use of moment closure techniques*, Theoretical Population Biology, **65** (2004), 49–65.
[19] J. H. Matis and T. Kiffe, "Stochastic Population Models," Springer, New York, Berlin and Heidelberg, 2000.
[20] M. N. Matrosovich, T. Y. Matrosovich, T. Gray, N. A. Roberts and H. D. Klenk, *Human and avian influenza viruses target different cell types in cultures of human airway epithelium*, Proceedings of the National Academy of Sciences, **101** (2004), 4620–4624.
[21] M. A. Nowak and R. M. May, "Virus Dynamics," Oxford Univ. Press, New York, 2000.
[22] B. Øksendal, "Stochastic Differential Equations: An Introduction with Applications," Springer, Verlag, Berlin, Heidelberg, $5^{th}$ edition, 2000.
[23] J. E. Pearson, P. Krapivsky and A. S. Perelson, *Stochastic theory of early viral infection: continuous versus burst production of virions*, PLoS Computational Biology, **7** (2011), 1–17.
[24] A. S. Perelson, D. E. Kirschner and R. De Boer, *Dynamics of HIV infection of CD4+ T cells*, Mathematical Biosciences, **114** (1993), 81–125.
[25] A. S. Perelson and P. W. Nelson, *Mathematical analysis of HIV-1 dynamics in vivo*, SIAM Review, **41** (1999), 3–44.
[26] A. N. Phillips, *Reduction of HIV concentration during acute infection: independence from a specific immune response*, Science, **271** (1996), 497–499.
[27] M. G. Roberts and J. Heesterbeek, *A new method to estimate the effort required to control an infectious disease*, Proceedings of the Royal Society London B, **270** (2003), 1359–1364.
[28] A. Singh and J. P. Hespanha, *Moment closure techniques for stochastic models in population biology*, Proceedings of the 2006 American Control Conference, (2006), 4730–4735.
[29] W. Y. Tan and H. Wu, *Stochastic modeling of the dynamics of CD4+ T-cells infection by HIV and some Monte-Carlo studies*, Mathematical Biosciences, **147** (1998), 173–205
[30] H. Tuckwell and F. Wan, *First passage time to detection in stochastic population dynamical models for HIV-1*, Applied Mathematics Letters, **13** (2000), 79–83.
[31] H. C. Tuckwell and E. Le Corfec, *A stochastic model for early HIV-1 population dynamics*, Journal of Theoretical Biology, **195** (1998), 451–463.
[32] P. van den Driesssche and J. Watmough, *Reproduction numbers and subthreshold endemic equilibria for compartmental models of disease transmission*, Mathematical Biosciences, **180** (2002), 29–48.
[33] P. van den Driesssche and J. Watmough, *Chapter 6: Further notes on the basic reproduction number*, in "Mathematical Epidemiology" (eds. F. Brauer, P. van den Driessche and J. Wu), Springer, Verlag, Berlin, Heidelberg, (2008), 159–178.
[34] F. Verhulst, "Nonlinear Differential Equations and Dynamical Systems," Springer-Verlag, Berlin, Heidelberg, New York, 1985.
[35] S. W. Vidurupola, "Deterministic and Stochastic Models for Early Viral Infection within a Host," M. S. Thesis, Texas Tech University, Lubbock, Texas, U.S.A., 2010.
[36] D. Wodarz and M. A. Nowak, *Mathematical models of HIV pathogenesis and treatment*, BioEssays, **24** (2002), 1178–1187.
[37] Y. Yuan and L. J. S. Allen, *Stochastic models for virus and immune system dynamics*, Mathematical Biosciences, **234** (2011), 84–94.
[38] S. R. Zaki, P. W. Greer, L. M. Coffield, C. S. Goldsmith, K. B. Nolte, K. Foucar, R. M. Feddersen, R. E. Zumwalt, G. L. Miller, A. S. Khan, P. E. Rollin, T. G. Ksiazek, S. T. Nichol, B. W. J. Mahy and C. J. Peters, *Hantavirus pulmonary syndrome: Pathogenesis of an emerging infectious disease*, American Journal of Pathology, **146** (1995), 552–578.

Received September 26, 2011; Accepted June 14, 2012.

*E-mail address*: sukhitha.vidurupola@ttu.edu
*E-mail address*: linda.j.allen@ttu.edu